Inactive   26 MAY 1948

NACA

RESEARCH MEMORANDUM

for the

Bureau of Aeronautics, Department of the Navy

AIR-FLOW CHARACTERISTICS OF FULL-SCALE DUCTS

FOR THE GRUMMAN XF9F-2 AIRPLANE

TED NO. NACA PP-302

By

Robert C. Spencer and Charles C. Wood

Langley Memorial Aeronautical Laboratory
Langley Field, Va.

NATIONAL ADVISORY COMMITTEE
FOR AERONAUTICS
WASHINGTON

NASA Technical Library

3 1176 01438 5240

NATIONAL ADVISORY COMMITTEE FOR AERONAUTICS

RESEARCH MEMORANDUM

for the

Bureau of Aeronautics, Department of the Navy

AIR-FLOW CHARACTERISTICS OF FULL-SCALE DUCTS

FOR THE GRUMMAN XF9F-2 AIRPLANE

TED NO. NACA PP-302

By Robert C. Spencer and Charles C. Wood

SUMMARY

An investigation has been made of the internal-flow characteristics of a full-scale mock-up of the induction air system for the Grumman XF9F-2 airplane. The purpose of the investigation was to determine the duct losses and reduce them if possible; secondary objectives were to determine the effects of fuselage boundary layer, the losses caused by a truss structure at the duct exit, and the magnitude of any surging or coupling effects between the two ducts.

The losses from inlet to the end of the duct proper were measured as about 12 percent of inlet dynamic pressure at an air flow of 100 pounds per second, which is near the high-speed condition. The losses from inlet to plenum chamber amounted to 28 percent of inlet dynamic pressure under the same conditions.

It was found possible to reduce the over-all losses in the duct system by refairing the lines of the inboard surfaces of the duct. The losses in the duct proper were reduced to slightly more than 9 percent of the inlet dynamic pressure, and the losses from inlet to plenum chamber were reduced to 26 percent of inlet dynamic pressure.

Boundary layers of $\frac{3}{4}$-inch and $1\frac{1}{2}$-inch thickness, created by introduction of a spoiler, caused increases in the over-all losses from inlet to plenum chamber of about 2 percent and 5 percent, respectively, of inlet dynamic pressure at a high rate of air weight flow. No evidence was found to indicate that the boundary layer caused increased irregularity in the flow.

A truss structure at the exit, made of tubing having a circular cross section, caused a negligible increase in the losses from inlet to plenum chamber.

A nonperiodic, small-magnitude fluctuation in the relative inlet velocities for the two sides of the system was observed. The average magnitude of the fluctuation was about 3 percent of the average dynamic pressure at the inlet and the maximum was about 10 percent of the inlet dynamic pressure.

INTRODUCTION

At the request of the Bureau of Aeronautics, Department of the Navy, an investigation has been conducted in the Langley induction aerodynamics laboratory to determine the air-flow characteristics of a full-scale mock-up of the engine air induction system for the Grumman XF9F-2 airplane.

The primary purpose of the investigation was to measure the duct losses and to make such modifications as were necessary to reduce the losses to the lowest practicable minimum. Secondary objectives were to determine the pressure distribution around the engine air screens, the effects of a boundary layer along the side of the duct adjacent to the fuselage, the losses caused by a tubular steel truss at the duct exit, and to detect and correct any excessive oscillatory or resonance effects arising from the duct geometry, as distinct from instabilities originating from external-flow conditions or the ingestion of fuselage boundary layer.

Modifications to the ducts included refairings along the inboard and outboard wall surfaces and the use of vanes, both near the inlet and at the exit of the duct. The range of air flows covered by the investigation was from about 10 to 110 pounds per second, in terms of the flow through both ducts.

APPARATUS AND METHODS

The XF9F-2 airplane is a single-engine jet-propelled fighter powered by a Rolls-Royce Nene engine. The engine air enters the airplane through wing-root inlets and is diffused through two ducts to a common plenum chamber containing the engine. The locations of the inlets, ducts, and plenum chamber in the airplane are shown in figure 1; the lines of the ducts and the plenum chamber, indicated by the dashed lines, are only approximate. The maximum-air-flow requirement for the engine was 112.3 pounds per second at top speed at sea level.

Description of basic model.- The ducts, built by the Grumman Aircraft Engineering Corporation and instrumented by the National Advisory Committee for Aeronautics, were of aluminum with wooden supporting structure.

A general view of the setup is shown in figure 2. The duct system consisted of two ducts, one right-hand duct and one left-hand duct, dumping into a common plenum chamber containing the mock-up of the engine. Figure 3 shows plan and elevation views of the duct lines and plenum chamber with the outlines of the engine mock-up also indicated. Station numbers as given in figure 3, and used subsequently in the paper, refer to inches aft of the nose of the airplane. As shown in figure 3, each duct was fitted with an entrance bell, designed to provide a uniform velocity profile across the inlet during the induced-flow tests. The bell, of course, would not be used in flight. The bell section was terminated approximately at station 195, which was the minimum section and was located at the mean position of the inlet station on the airplane. Diffusion of the air begins at station 195 and continues to station 258, where, as shown in figure 3, one side of the duct is open to the plenum chamber so that a large portion of the air is effectively dumped at that station. The area ratio of the outlet (station 258) to the inlet (station 195) was approximately 2.68, and the equivalent conical angle of expansion was about 9°. Figure 4 shows sections of the duct at various stations; tables of radii and center locations are included for reference. The duct assembly was divided along the plane of symmetry, as shown in figure 5, to provide easy accessibility for instrumentation and modification of the ducts. The engine mock-up was also divided at the center plane. Either half of the assembly, therefore, could be tested separately by bolting a large wooden cover over the open plenum chamber. The setup in such cases thus consisted of either the right- or left-hand duct and half of the plenum chamber, containing half of the engine. Such an arrangement made it possible to test either half separately while the other half was being modified.

Duct modifications.- Several modifications to the internal duct lines were made in attempts to reduce total-pressure losses ahead of the plenum chamber and also to improve the velocity distribution at the point where the air was dumped into the plenum chamber.

First attempts at modification of the duct lines were made using modeling clay. The internal lines of the duct were altered by several different fairings, both forward and aft of station 220 (fig. 3), and the intake bell was also completely reworked by means of the clay. None of the above fairings was successful; therefore, a more extensive fairing was laid out modifying the duct contour along the inboard wall as shown in figures 6 and 7. The fairing was composed of an industrial gypsum plaster applied to the inner wall of the duct and then worked down carefully to the desired lines. A photograph of the installation is shown as figure 8. The feathering of the edge of the plaster into the original metal lines was such that no break could be detected in the smoothness of the surface. The new duct lines maintained the original method of layout, using circular arcs joined by straight lines. The refairing was accomplished by using different radii and relocating the centers.

A second revision of the duct lines consisted of a sheetmetal refairing of the outboard wall to ease the bend at the rearward section of the duct; the fairing was supplied by the Grumman Company and was installed by the NACA in the starboard duct after the duct had been refaired on the inboard wall with plaster. A photograph of this installation is shown as figure 9.

Attempts were also made to control separation aft of station 220 and to improve the velocity distribution at the dumping point by use of vanes. As a first attempt, a simple horizontal vane was installed at the bend at station 220. This vane is shown in figure 10. Subsequently, the slanted vane shown in figure 11 was installed and was tested separately and in conjunction with turning vanes at the aft end of the duct. The slanted vane intersected the floor at an angle of about 80°, and the vane span was 13 inches at station 220. Both the horizontal and slanted vanes were installed in the starboard duct in its original condition.

Turning vanes were also employed in conjunction with the plaster fairing shown in figures 6 to 8. Photographs of the vane installation are shown as figures 12 and 13. The general appearance of these vanes was the same as that of the turning vanes that were used in conjunction with the aforementioned slanted vane. An additional set of turning vanes, which was tried in conjunction with the inboard plaster fairing, was laid out in such a manner that the passages inboard of the vanes underwent no expansion in the bend. This was accomplished by neglecting the outboard section of the duct (fig. 13) and allowing that portion to undergo a very large expansion downstream of the bend in hopes of attaining an over-all improvement by a large improvement in the flow through the center and inboard portions of the duct.

Revised estimates of the structural requirements of the airplane during the period of these tests indicated the need for the installation of three truss members across the duct at the entrance to the plenum chamber. These members were of tubing having a circular cross section and having outside diameters of $1\frac{1}{2}$-inches, $1\frac{1}{8}$-inches, and 1 inch. Determination of the effect of a mock-up of this truss structure (fig. 14) upon the over-all loss to the plenum chamber was made during the latter part of the test program.

Boundary layer.- In order to investigate possible disturbing effects of ingestion of fuselage boundary layer, the intake bell was modified by extending the inboard section by means of a flat plate, and a spoiler was installed on the plate to generate a boundary layer ahead of the inlet. Two arbitrary thicknesses of boundary layer were investigated: one of $1\frac{1}{2}$-inches and one of $\frac{3}{4}$-inch thickness at the inlet. The total thickness

was measured by a rake of small total-pressure tubes closely spaced, installed at station 195. A survey was made also at a point 7 inches downstream from station 195 to determine whether incipient separation might be occurring at the inlet station.

Instrumentation.- Air flow through the setup was measured by means of a calibrated screened venturi located downstream of the model.

Static pressure at the inlet was measured by three static-pressure orifices located at the midpoints of the flat sections at station 195. (See fig. 4(a).)

Pressures at station 258 were measured by 8 static-pressure orifices and 14 shielded total-pressure tubes located as shown in figure 15. Both ducts were instrumented at this station. In addition to the instrumentation at station 258, total-pressure measurements were made on the starboard duct at the intersection of the duct with the plenum chamber, where three rakes of three tubes each were installed. These rakes can be seen in the photographs of figures 5 and 12.

Pressures at the plenum chamber were measured by four tubes, essentially sheltered static-pressure tubes, located in sheltered corners at the top and bottom of the two halves of the chamber at station 260. The two top tubes are visible in figure 5. Additional static-pressure tubes were located in the plenum chamber near the top and bottom of the port half of the plenum chamber at about stations 270 and 290, respectively. These latter tubes were installed to check the validity of the readings from the sheltered tubes at station 260.

Pressure distribution over the engine screens was measured by 10 shielded total-pressure tubes at each of the two screens. Figure 16 is a photograph of the installation on the port half of the engine mock-up and figure 17 shows the locations of the tubes around the screens.

Methods and tests.- Air flow was induced by connecting the setup to the suction side of a 1000-horsepower blower. Preliminary investigations were first carried out using tufts on the duct wall and tufts on a hand-held survey rod to determine the character of the air flow.

The inlet dynamic pressure q_i was computed from the venturi weight flow measurements and the inlet area.

The average total-pressure loss $\dfrac{\Delta H}{q_i}$ to station 258 was determined by plotting the losses at each of the 14 total-pressure tubes (measured as the difference between the total pressure at the tube and atmospheric pressure) on a section drawing of the station and integrating the contours of constant $\dfrac{\Delta H}{q_i}$ determined by the plots.

Plenum-chamber total-pressure losses were measured as the difference between the arithmetic average of the sheltered static-pressure tubes and atmospheric pressure and were expressed as $\frac{\Delta H}{q_i}$.

It was suspected that the air entering the plenum chamber from the two ducts, instead of diffusing immediately and losing its kinetic energy, continued onward as a jet and impinged at high velocity, without total-pressure loss, on localized areas of the engine air intake screens. An attempt was therefore made to get an idea of the importance of the effect, although neither the faithfulness of reproduction of the engine in the mock-up nor the extent of the instrumentation was sufficient to permit accurate determinations. The method employed in estimating the mass-flow-weighted mean total pressure at the engine inlet screen was based upon the assumption of uniform static pressure at the screens. This pressure had not been measured and was arrived at by selecting a value which, in conjunction with the measured engine inlet screen total pressures, gave a calculated engine air flow equal to that measured by the venturi. Inlet velocities were then calculated from the static pressure and from the measured engine inlet total pressures. The weighted mean total pressure at the inlet was then calculated from the calculated velocities and the measured total pressures. Throughout the calculations integration methods similar in principle to those explained in reference 1 were employed.

Coupling effects were determined by manifolding the three static-pressure orifices in each inlet and connecting to the opposite sides of a U-tube. Any difference in the flow through the ducts, caused by resonance or oscillatory tendencies between the two ducts, was indicated by a difference in the level of the two sides of the manometer.

The effect of installation of a water tank and a hydraulic tank in the plenum chamber was determined by installing mock-ups of the tanks in the plenum chamber and operating with the complete duct.

RESULTS AND DISCUSSION

The results of this investigation are summarized in Table I. It should be noted that most of the data are for an air-flow rate of 85 pounds per second, because many of the less-promising modifications were not taken to the highest flow rates obtainable. Most of the results summarized in the table and described subsequently in the paper are for tests with only one duct (either port or starboard) and half of the plenum chamber and engine. For convenience, such a setup will be referred to as a "half-duct." When both ducts were in operation, the setup will be referred to as a "complete duct."

Original condition.- Complete data taken with the port duct in the original condition are presented in figure 18. It is seen from the figure that the diffuser loss coefficient was approximately doubled to 12 percent of the inlet dynamic pressure when the air-flow rate was increased from 20 to 50 pounds per second. Calculated loss for a smooth conical duct of equivalent expansion ratio and diffuser angle is 7.1 percent of q_i (reference 2). (The calculation does not indicate a variation with flow rate.) Preliminary surveys with wall tufts had shown that the flow separated from the inboard wall and along the floor of the duct aft of station 220. This separation undoubtedly accounts for the greater part of the excess diffuser loss. The dumping loss from station 258 into the plenum chamber was calculated as $0.14q_i$ by assuming all the kinetic energy was lost at station 258; the measured loss was $0.16q_i$ at an air-flow rate of 50 pounds per second for the half-duct.

The upper curve of figure 18 shows the losses from inlet to plenum chamber. The general trend of the curve is similar to that of the curve for the diffuser loss (to station 258).

Duct modifications.- Data showing the effects of the various revisions of the duct are presented in figures 19 to 24. The diffuser loss with the inboard plaster fairing alone is shown in figure 19 to have been appreciably lower at the high flow rates than the loss for the original configuration. The general characteristic of the two curves, however, is the same, the improvement effected by the refairing having been obtained as a result of the delay in the point at which the losses increased with air flow. The pressure loss to the plenum chamber with the refaired inboard wall is shown in figure 19 to increase slowly at air flows above 32 pounds per second; whereas the loss with the original configuration increased at a greater rate for air flows greater than 24 pounds per second. Typical pressure contours at station 258 are presented in figure 20 for both of these configurations. Tests of the complete system in both the original and refaired conditions are presented in figure 21. The maximum flow induced through the system with both ducts was about 85 pounds per second. Data from the half-duct tests were used to extrapolate the curves to flow rates above 100 pounds per second by multiplying the observed flow rates for the half-duct by 2 in order to make the data comparable to those from the complete duct. Because of the presence of the solid wall in the plane of symmetry, for the half-duct, the variation in losses with air weight flow for the half-duct installation differed from that for the complete duct. This wall is not considered to have in any way affected the determination of the relative merits of the various modifications.

Mock-ups of the hydraulic tank and the water tank were received during the progress of the investigation and were installed in the plenum chamber after both ducts had been refaired with plaster along the inboard walls. As shown in figure 22, the installation caused a slight increase in the losses at the plenum chamber.

The effect of the metal fairing for the outboard wall of the duct is shown in figure 23. Losses at station 258 were not measured for this configuration, as to do so would have involved reinstrumentation of station 258. It is believed that the comparatively large adverse effect of the metal fairing is the result of the decreased cross-sectional area of the duct which increased the velocity of the air dumped into the plenum chamber.

In figure 24 are shown the results of other modifications that were tried. Data are not shown for the combination of the inboard plaster fairing with turning vanes at the exit, because severe vibration of the vanes prevented the taking of complete data. It is seen from figure 24 that the combination of the slanted vane with turning vanes at the duct exit gave favorable results at high flow rates. In this case, however, the vibration of the turning vanes was very severe. Careful realinement of the vanes with the air flow (by means of tuft observations) gave no apparent decrease in the vibration.

Effect of inlet boundary layer.- The results of a series of tests with an artificially created boundary layer along the inboard wall of the starboard duct are presented in figures 25 and 26. Figure 25 shows the velocity profile of the $1\frac{1}{2}$-inch boundary layer at station 195; the symbols y, δ^*, u, and u_0 refer to the distance of the survey tube from the wall, the boundary-layer displacement thickness $\left[\int_0^\infty \left(1 - \frac{u}{u_0}\right) dy\right]$, the velocity at the survey point, and the stream velocity outside the boundary layer, respectively. The total boundary-layer thickness, used to specify the boundary layers, is defined as the maximum distance from the wall at which a measurable reduction in total pressure occurred. It will be seen from the figure that changes in the mass flow caused very little change in the velocity profile; the actual range of mass flows was from about 15 pounds per second to 85 pounds per second.

The effects of the $\frac{3}{4}$-inch and $1\frac{1}{2}$-inch boundary layers upon the pressure recovery are shown in figure 26. This investigation was made with the modified duct with the refaired inboard wall, only. The data showed that the pressure loss to the plenum chamber increased with boundary-layer thickness, from a value of approximately 26 percent of q_i with a minimum boundary-layer condition to 28 percent for the $\frac{3}{4}$-inch and 31 percent in the $1\frac{1}{2}$-inch boundary layer at an air-flow rate of 50 pounds per second. Estimates for the $1\frac{1}{2}$-inch boundary layer indicated that approximately one-fourth of the increase in pressure loss at the plenum chamber might be attributed to loss ahead of the inlet station, incurred in generating the thickened boundary layer. The general character of the pressure-loss variation with air flow was unaffected by the presence of the boundary layer.

Effect of structural members.- Data taken on pressure losses to the plenum chamber with the truss installed (fig. 14) were measured in conjunction with the refaired duct inner wall. These data are presented in figure 27. The average loss was affected very little by the installation of the circular truss members.

Coupling.- Tests of the system, refaired with plaster, were made at several air flows to investigate any resonance effects that might result from the interaction of the two halves of the system. Although variations in velocity through each duct were observed, they showed no consistent pattern or frequency and were undoubtedly caused by local fluctuations in the flow pattern. The variations shown on the alcohol manometer were entirely irregular, consisting chiefly of very quick fluctuations in the manometer reading. At an inlet dynamic pressure of 315 pounds per square foot and an air-flow rate of 85 pounds per second, the amplitude of the fluctuations ranged from about 3 percent to about 10 percent of inlet dynamic pressure. The period of the fluctuations varied from 10 seconds to 2 minutes. The data therefore indicated that there was no inherent oscillatory tendency in the mock-up. Obviously, instabilities originating from external-flow conditions would not be present in this type of tests.

Pressure distribution and losses at engine screens.- None of the modifications that were tried had any appreciable effect upon the pressure-distribution pattern over the two engine air screens. The distribution with the inboard plaster fairing was selected as typical and is shown in figure 28 for a relatively high air flow. It will be seen from the figure that the pressures at the two sides of the front screen, where the air from the ducts impinges on the engine, are very nearly the same as atmospheric pressure. It is evident, therefore, that a portion of the air, instead of losing its kinetic energy at the dumping point, continues to the engine screen at high velocity.

The weighted total-pressure loss at the engine screens was evaluated by using the methods described in the section entitled "Methods and tests" together with the measured losses to station 258 and to the plenum chamber. This comparison is made at a total engine air flow of about 85 pounds per second and presented in the following table:

	Induction-system loss, $\dfrac{\Delta H}{q_i}$ (percent)	
	Original condition	Refaired on inboard wall
Ducted section (to station 258)	11	7
Loss to engine screens	25	18
Loss to plenum chamber	28	26

Inspection of the foregoing table shows that the induction-system loss based on estimated total-pressure recovery at the engine inlet is less than the loss based on plenum-chamber pressure measurements in both the original and refaired conditions, with a definite advantage for the refaired ducts. The determination of pressure loss coefficients from measurements by sheltered tubes in the plenum chamber is therefore probably on the conservative side. In both cases, the ratio of engine inlet loss to diffuser loss is about the same. Since the method of estimating the engine inlet total-pressure recovery is at best of strictly limited accuracy, the values obtained may be considered as qualitative only.

Application.- When the aforementioned results are considered in the light of applicability to the airplane, it should be borne in mind that the lines of flow ahead of the mock-up will differ from the lines of flow ahead of the inlets on the actual airplane in flight. Therefore, from the nature of the investigation, estimates of the effects of the measured losses upon the actual airplane performance should be limited to comparative estimates. For an assumed inlet velocity ratio of 0.5, the figure of 28 percent for the over-all loss to the plenum chamber becomes 7.0 percent in terms of free-stream dynamic pressure, and the differences between different configurations become correspondingly smaller.

CONCLUDING REMARKS

The results of the various investigations that were made may be summarized briefly as follows: In the original condition, the loss in the duct proper, at an air flow of 100 pounds per second, was measured as 12 percent of q_i. The loss from inlet to plenum chamber was 28 percent of q_i under the same conditions.

Refairing the duct lines along the inboard wall reduced the losses in the duct proper from a value of $\dfrac{\Delta H}{q_i}$ of 12 percent to a value of about 9 percent at air flows corresponding to the high-speed condition. The over-all loss from inlet to plenum chamber was reduced from a value of 28 percent to a value of 26 percent at an air flow of 100 pounds per second.

Artificially created boundary layers of $\frac{3}{4}$-inch and $1\frac{1}{2}$-inch thickness caused increases in the over-all losses from inlet to plenum chamber of 2 percent and 5 percent, respectively, of inlet dynamic pressure, at an air-flow rate of 100 pounds per second.

A truss at the exit of the duct, consisting of three members having circular cross sections of $1\frac{1}{2}$-inches, $1\frac{1}{8}$-inches, and 1 inch, caused negligible change in the over-all losses.

A nonperiodic, small-magnitude fluctuation in the relative inlet velocities for the two sides of the system was observed. The average magnitude of the fluctuation was about 3 percent of the dynamic pressure at the inlet, and the maximum observed was about 10 percent of the dynamic pressure at the inlet.

Langley Memorial Aeronautical Laboratory
        National Advisory Committee for Aeronautics
                Langley Field, Va.

Robert C. Spencer
Aeronautical Research Scientist

Charles C. Wood
Aeronautical Research Scientist

Approved:
        John V. Becker
Chief of Compressibility Research Division

RCM

REFERENCES

1. Nichols, Mark R.: An Experimental Investigation of the Intercooler and Charge-Air Duct Systems of the P-60A Airplane. NACA ACR No. 3J14, 1943.

2. Henry, John R.: Design of Power-Plant Installations. Pressure-Loss Characteristics of Duct Components. NACA ARR No. L4F26, 1944.

TABLE I

RESULTS OF DUCT MODIFICATIONS

[Tests were with the half-duct unless otherwise noted; air-flow
rates given are for the complete system of the two ducts]

Condition	Loss coefficient, $\frac{\Delta H}{q_i}$ (percent) to -			
	Station 258 (duct loss)		Plenum chamber	
	Air-flow rate (lb/sec)		Air-flow rate (lb/sec)	
	85	100	85	100
Original	10	12	[a]28	28
Several revisions, refaired with modeling clay	10	---	[a]28	---
Plaster fairing, inboard	7	9	[a]26	26
Metal fairing, outboard, with inboard plaster fairing	--	---	30	---
Horizontal vane	10	---	30	---
Slanted vane	--	---	28	---
Slanted vane plus turning vanes	9	---	25	---
Inboard plaster fairing plus turning vanes	[b]--	[b]---	[b]--	[b]---

[a]Complete duct.
[b]Heavy flutter of vanes prevented extensive testing.

Plenum chamber

Ducts

Inlets
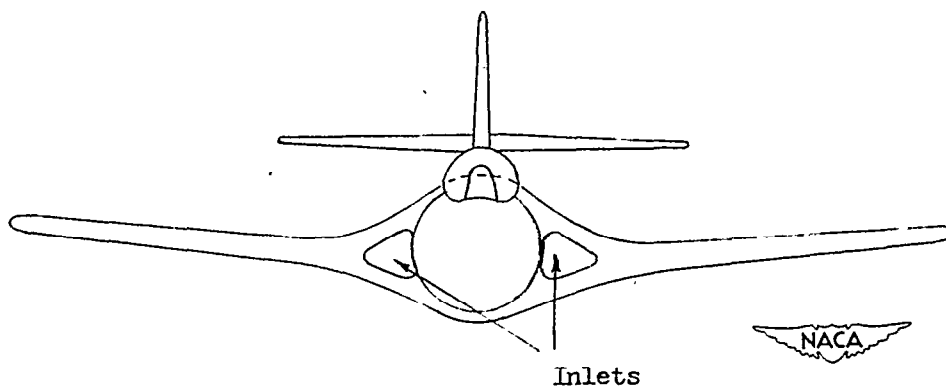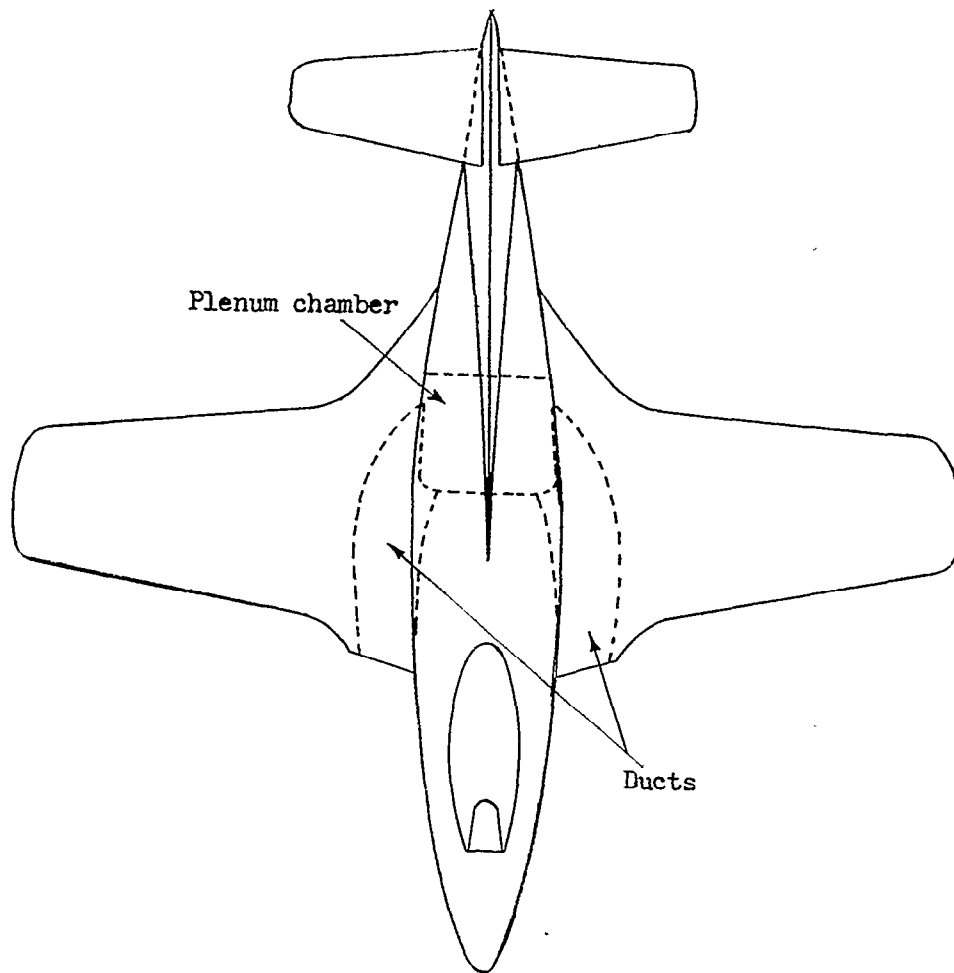
NACA

Figure 1.- Schematic diagram showing approximate locations of
ducts and plenum chamber in the XF9F-2 airplane.
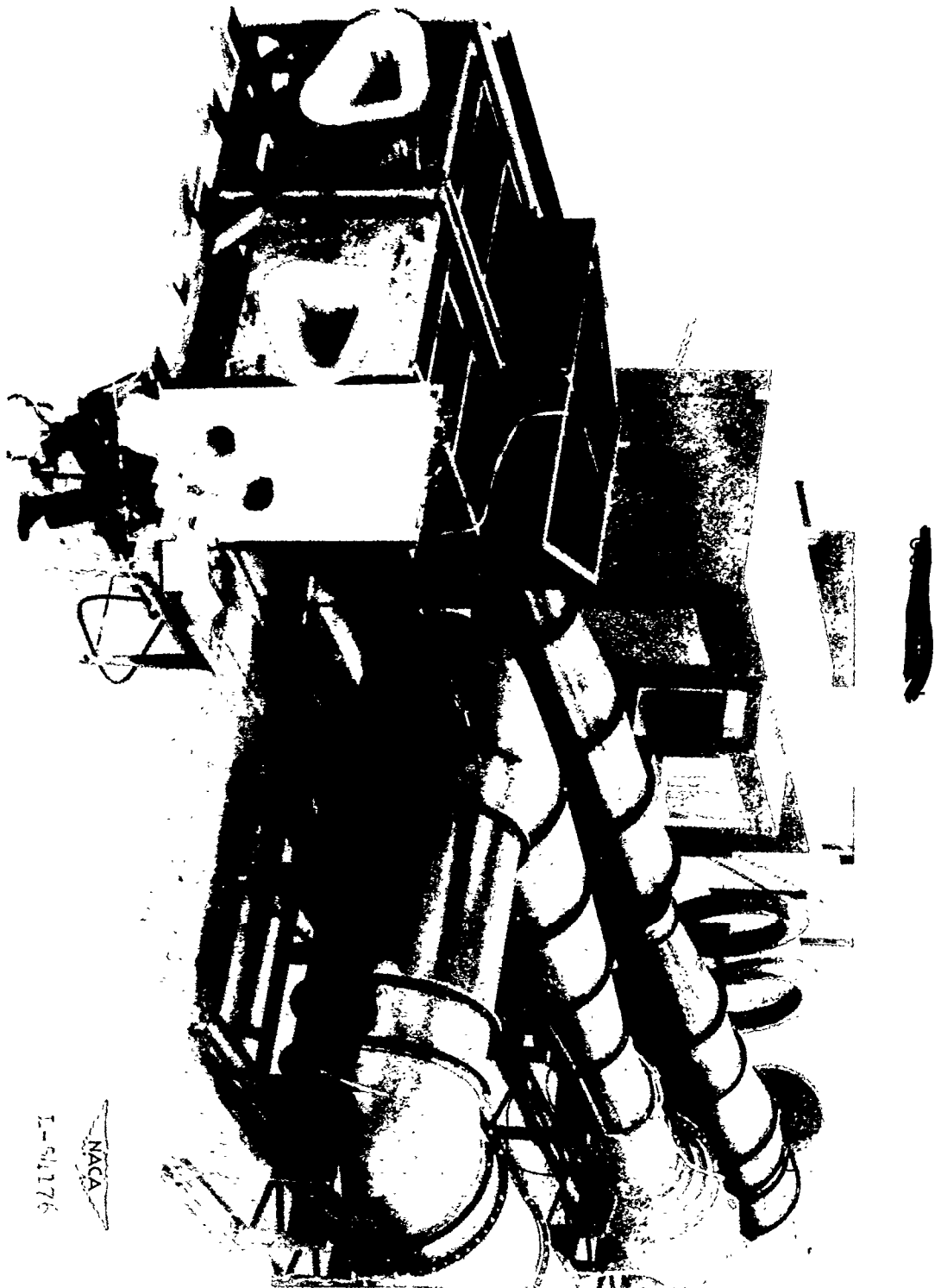
Figure 2.- General arrangement of test equipment.

L-64176
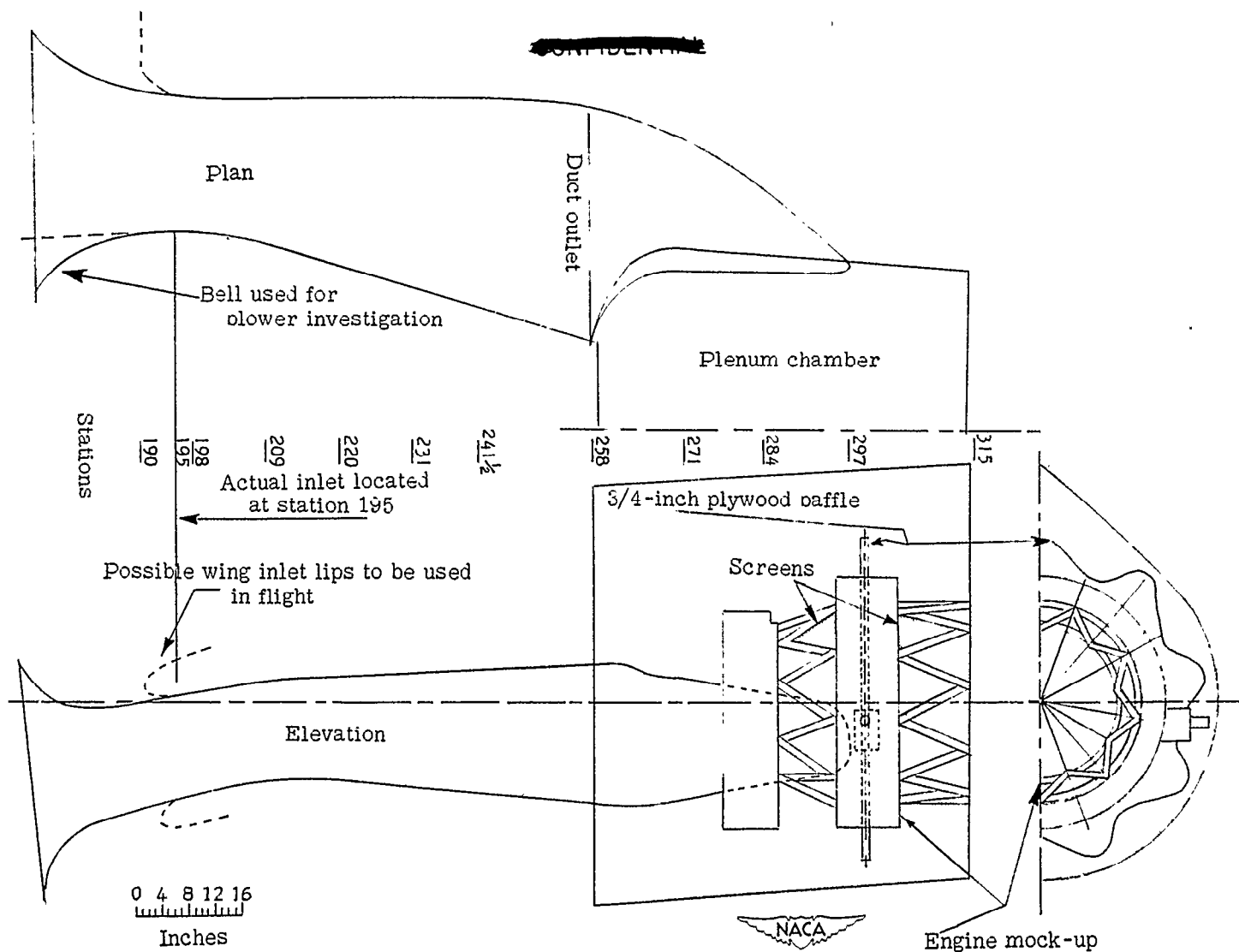
Figure 3.- Plan and elevation view of XF9F-2 engine-air inlet duct.

Station	Inboard R.	Outboard R. (One center)
195 Upper	15/16	2-11/16
198 Upper	2-1/4	2-15/16
203 Upper	4-7/16	3-5/16
209 Upper	6	3-1/2
214 Upper	7-1/8	3-9/16
217 Upper	7-1/2	3-9/16
220	7-3/4	3-9/16
217 Lower	7-3/8	
214 Lower	6-15/16	
209 Lower	5-5/8	
203 Lower	3-15/16	
198 Lower	1-9/16	
195 Lower	9/16	
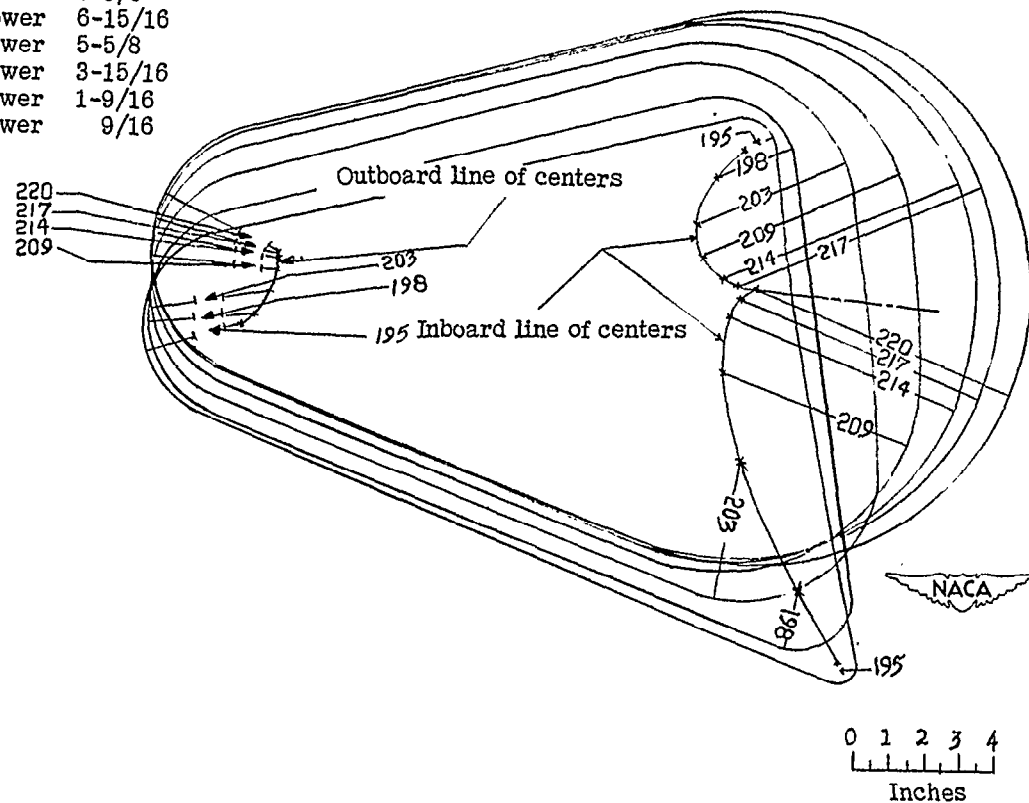
(a) Station 220 forward.

Figure 4.- Section view of XF9F-2 engine-air inlet duct.

CONFIDENTIAL

Station Outboard	Radius	Station's center from center of station 220	Station Inboard	Radius	Station's center from center of station 220
220	3-7/16	0	220	7-3/4	0
225-1/2	3-19/32	0	225	8-3/32	1-5/16
231	3-19/32	0	231	8-7/16	2-5/16
236-1/2	3-19/32	0	236	8-3/4	3-15/16
241-1/2	3-10/16		241	9-1/16	5-1/4
247	3-21/32		247	9-7/16	6-9/16
250	3-11/16		250	9-5/8	7-5/16
252-1/2	3-3/4		252	9-3/4	7-7/8
258	4	1	258	10-1/8	9-1/4
262-1/4	3-15/16	2			
266-3/4	3-9/16	3			
271	3-7/16	5			
275-1/4	3-9/16	7			
279-3/4	3-7/8	10			
284	4-5/16	14			
288-1/4	4-1/16	18			
292-3/4	6-1/4	24			

(b)   Station 220 aft.

Figure 4.- Concluded.

CONFIDENTIAL

Figure 5.- Duct system separated into two halves, showing plenum chamber.

Termination of fairing

Plaster fairing

Plenum chamber

Stations

190 198 209 220 231 247 258 271 284 297 315
    195

Actual duct begins at
this station.

Elevation

0 4 8 12 16
Inches
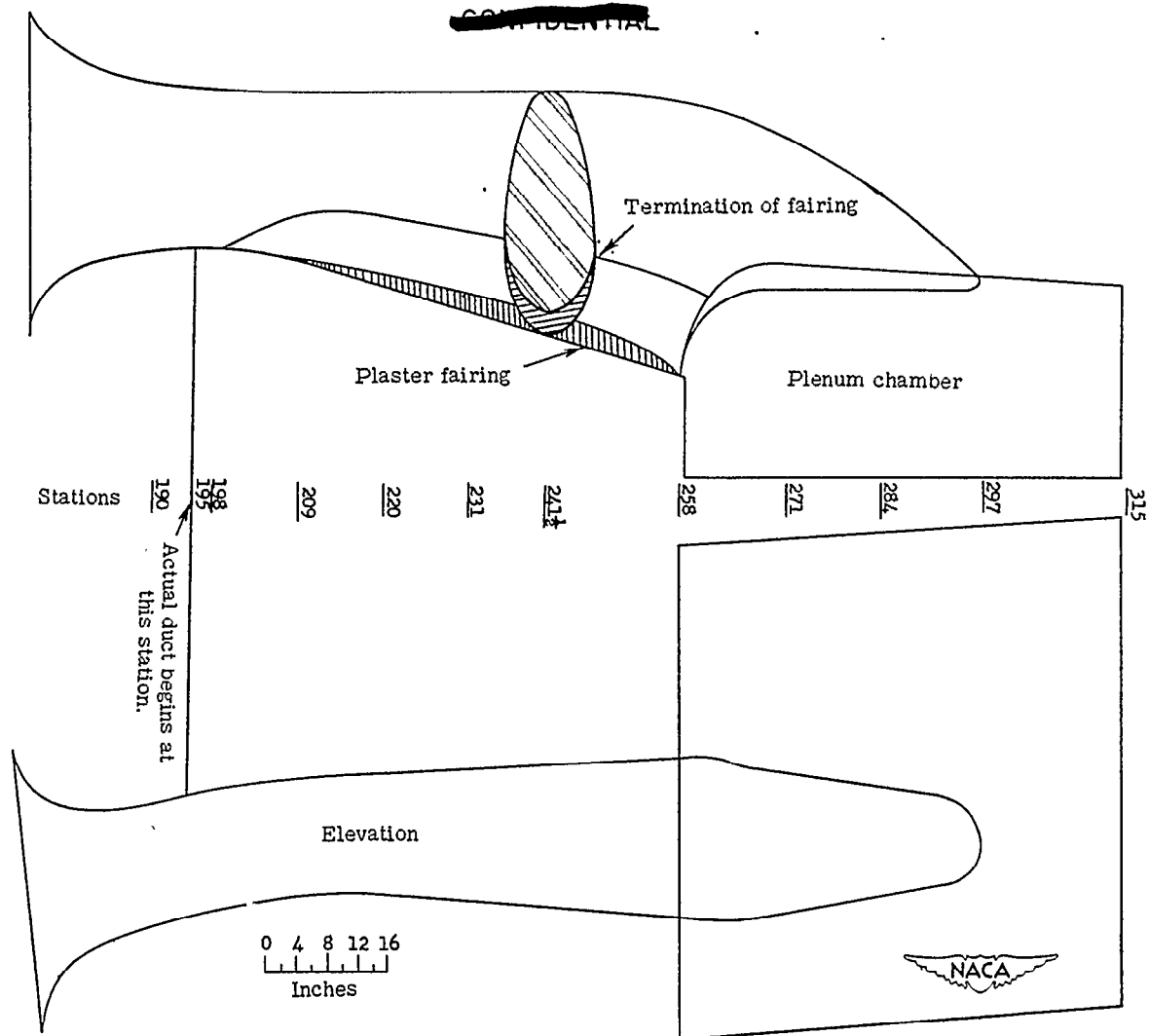
NACA

Figure 6.- Plan and elevation view of XF9F-2 engine-air inlet duct as refaired
along inboard wall.
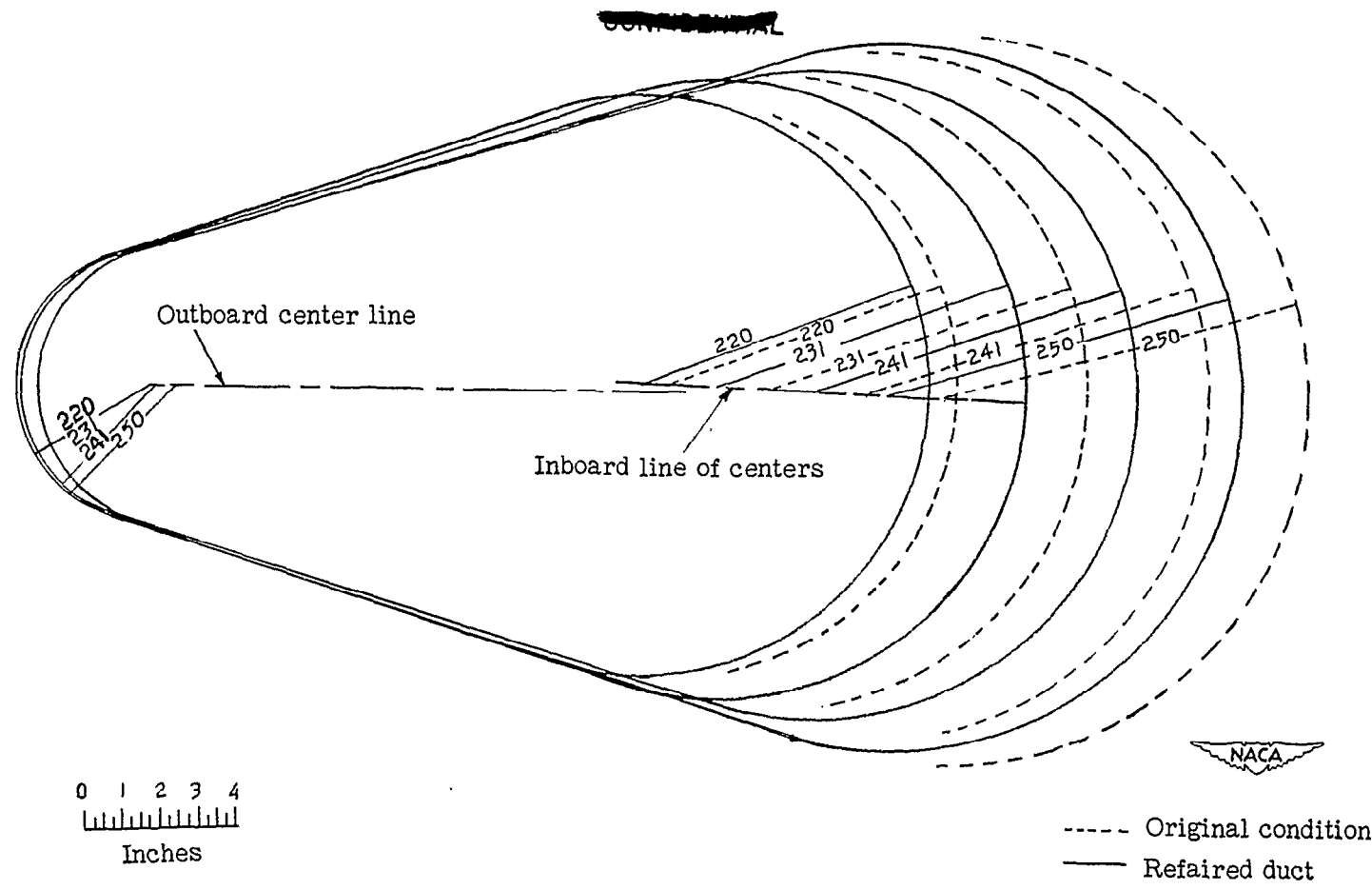
Figure 7.- Section view of XF9F-2 engine-air inlet duct as refaired along inboard wall.
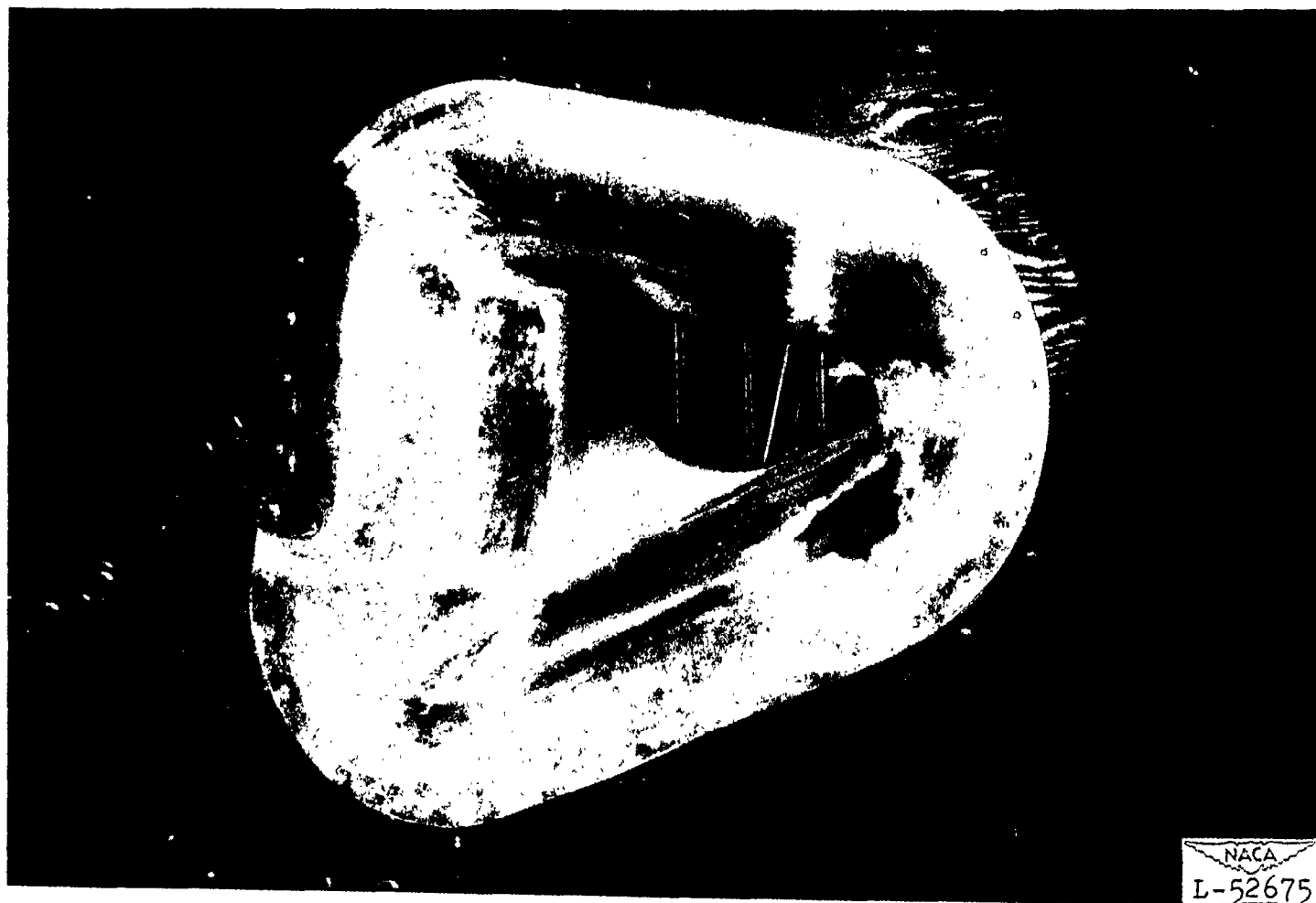
Figure 8.- Plaster fairing installed in inboard side of port duct.

Figure 9.- Metal fairing installed in outboard side of starboard duct.

L-52339

Figure 10.- Horizontal vane installed in starboard duct.

Figure 11.- Slanted vane installed in starboard duct.

Figure 12.- Turning vanes at exit of starboard duct. Viewed from plenum chamber.

L-52956

Figure 13.- Turning vanes at exit of starboard duct. Viewed from duct inlet.
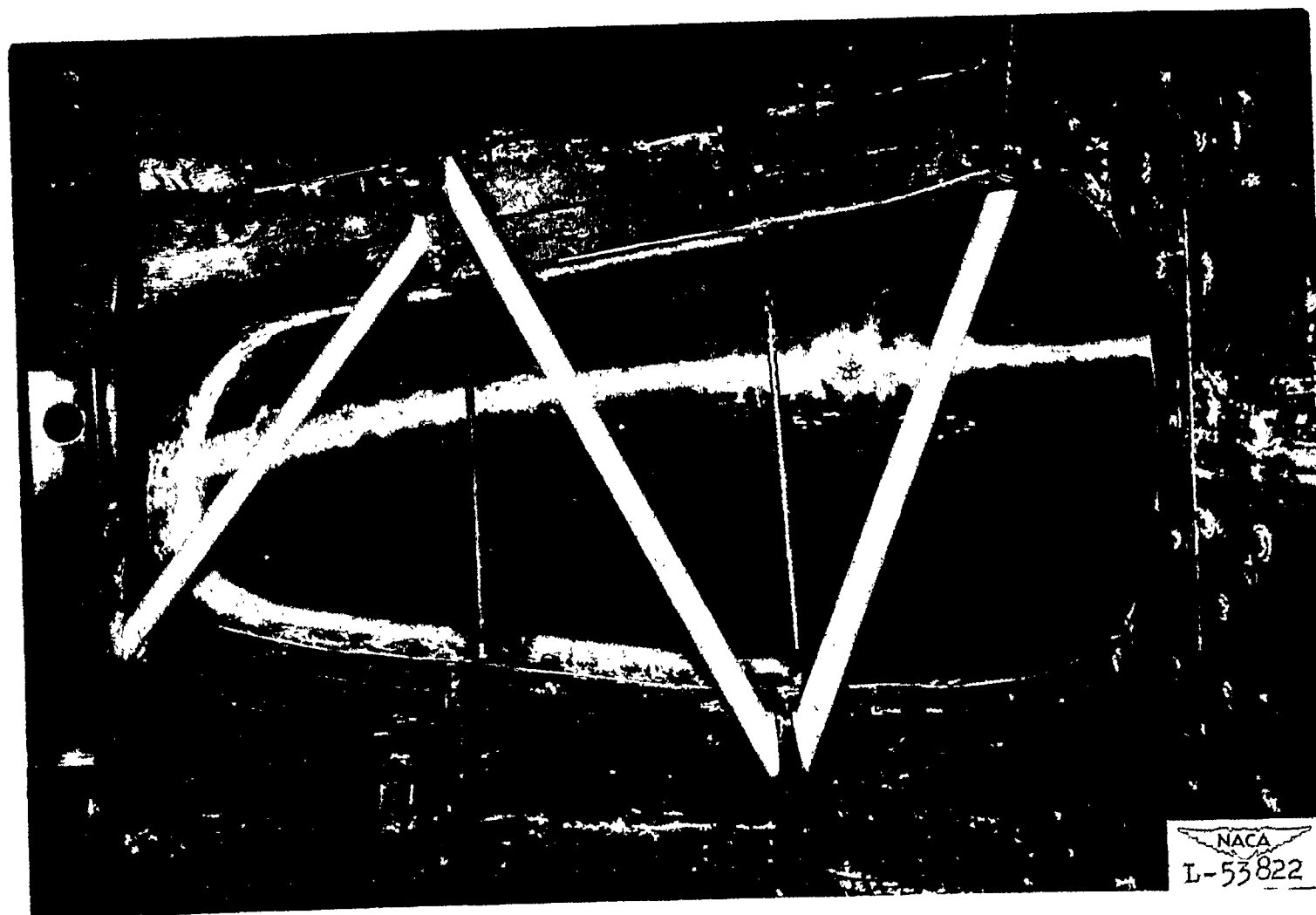
Figure 14.- Truss structure at exit of port duct.

0 1 2 3 4
Inches

⊙ | Shielded total-pressure tubes
⊗ | Wall static-pressure orifices
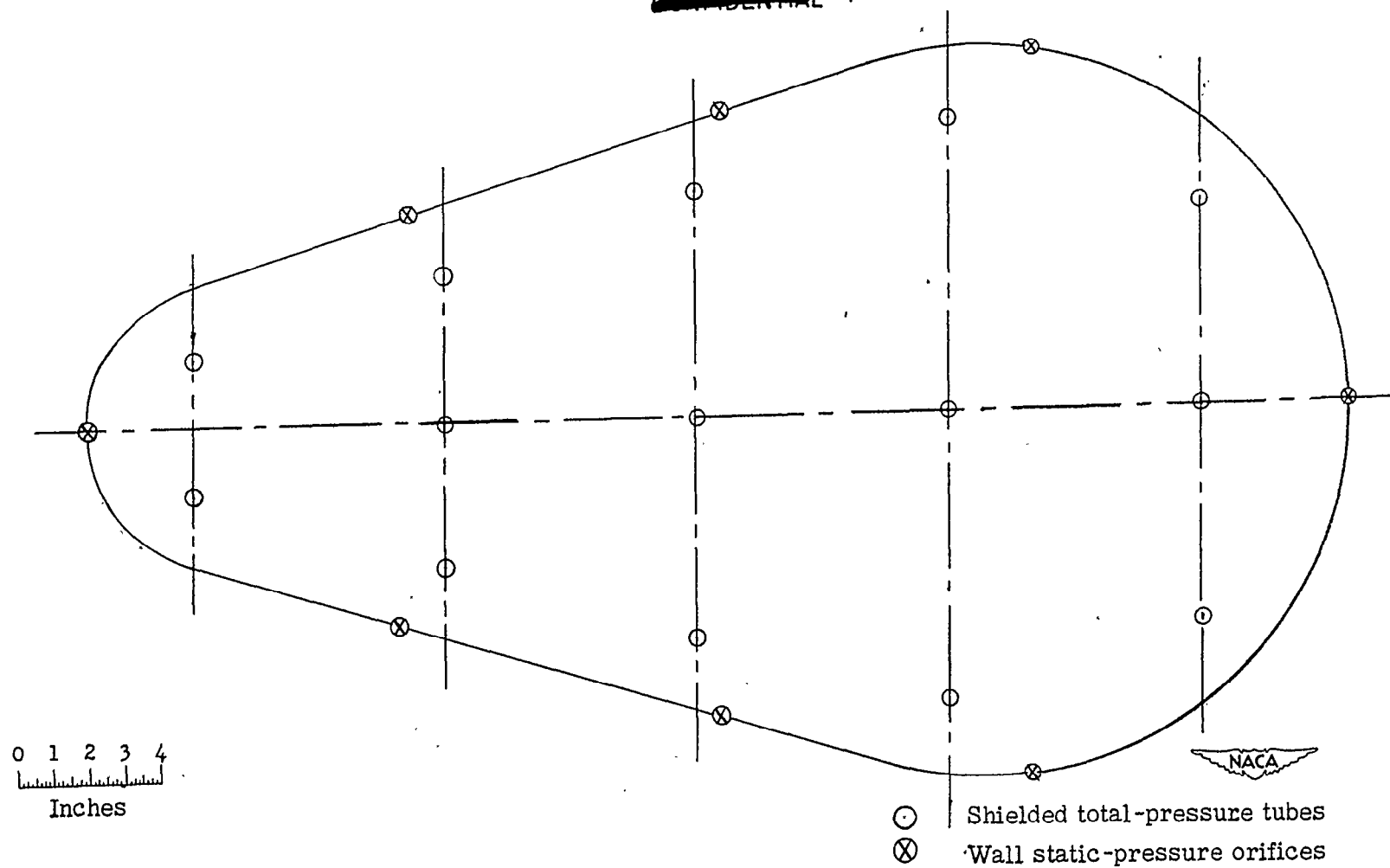
Figure 15.-   Instrumentation at duct exit (station 258).
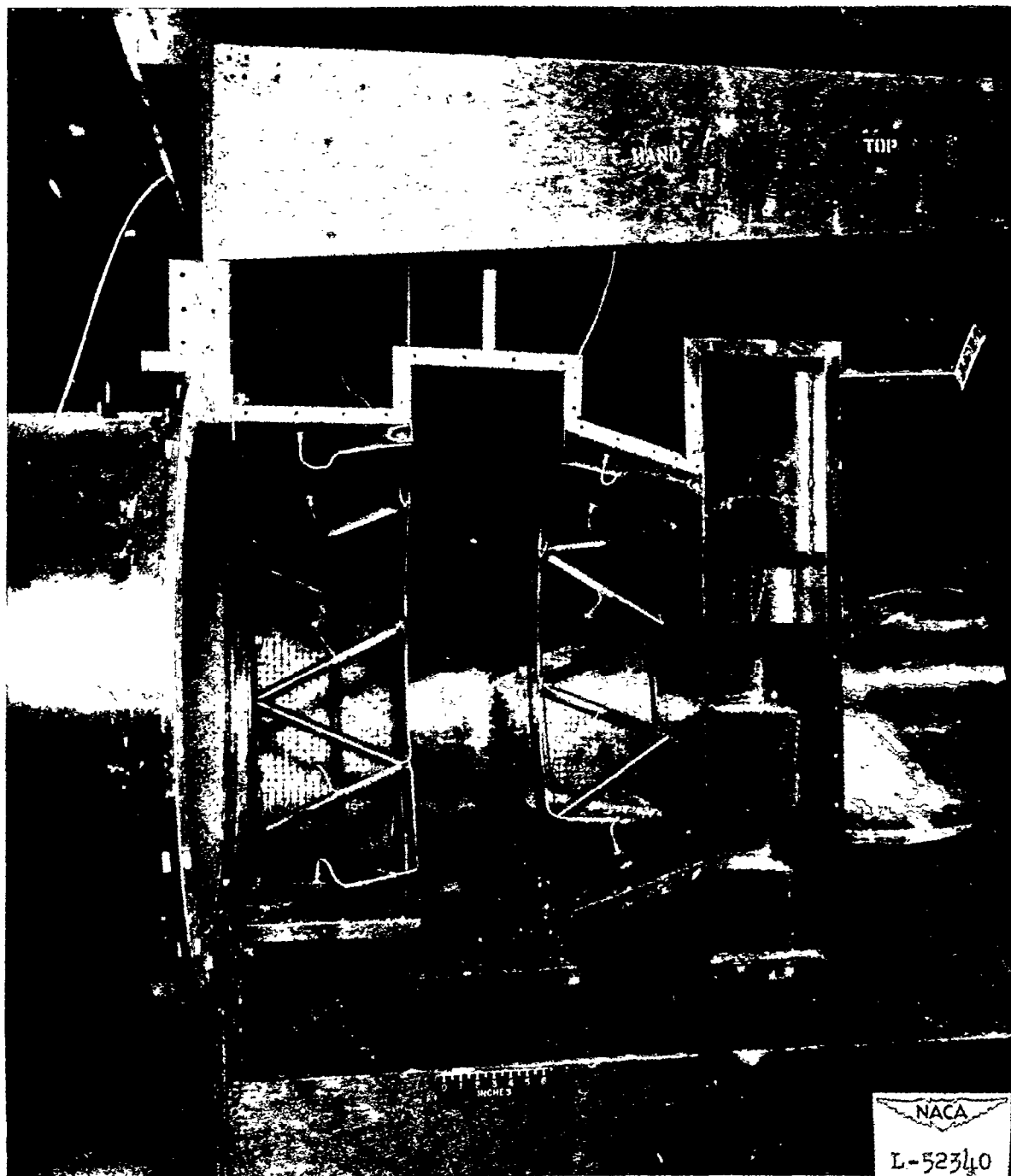
Figure 16.- Pressure-tube installation at engine screens.
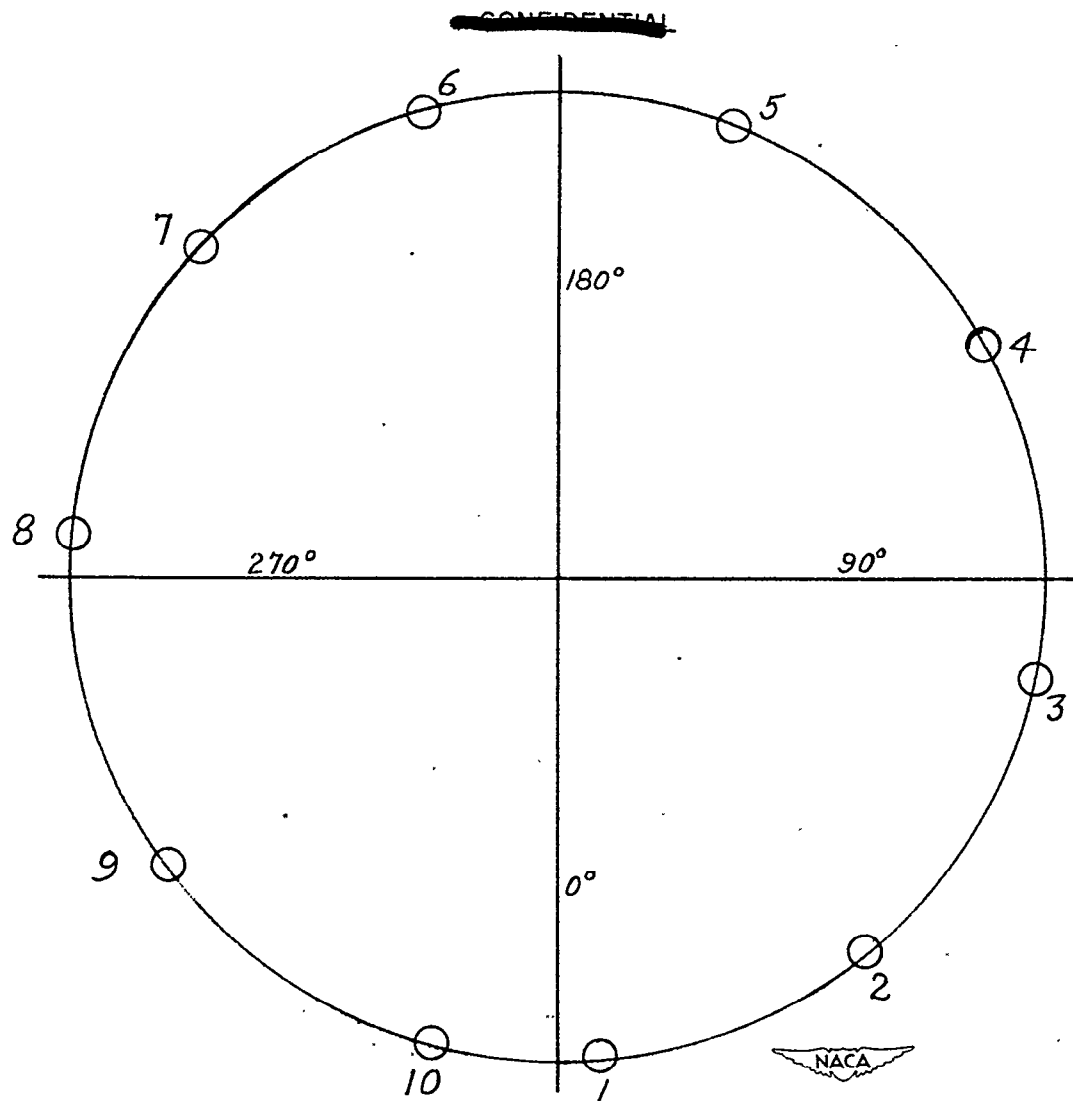
Figure 17.- Locations of total-pressure tubes at front and rear engine screens. Looking upstream.
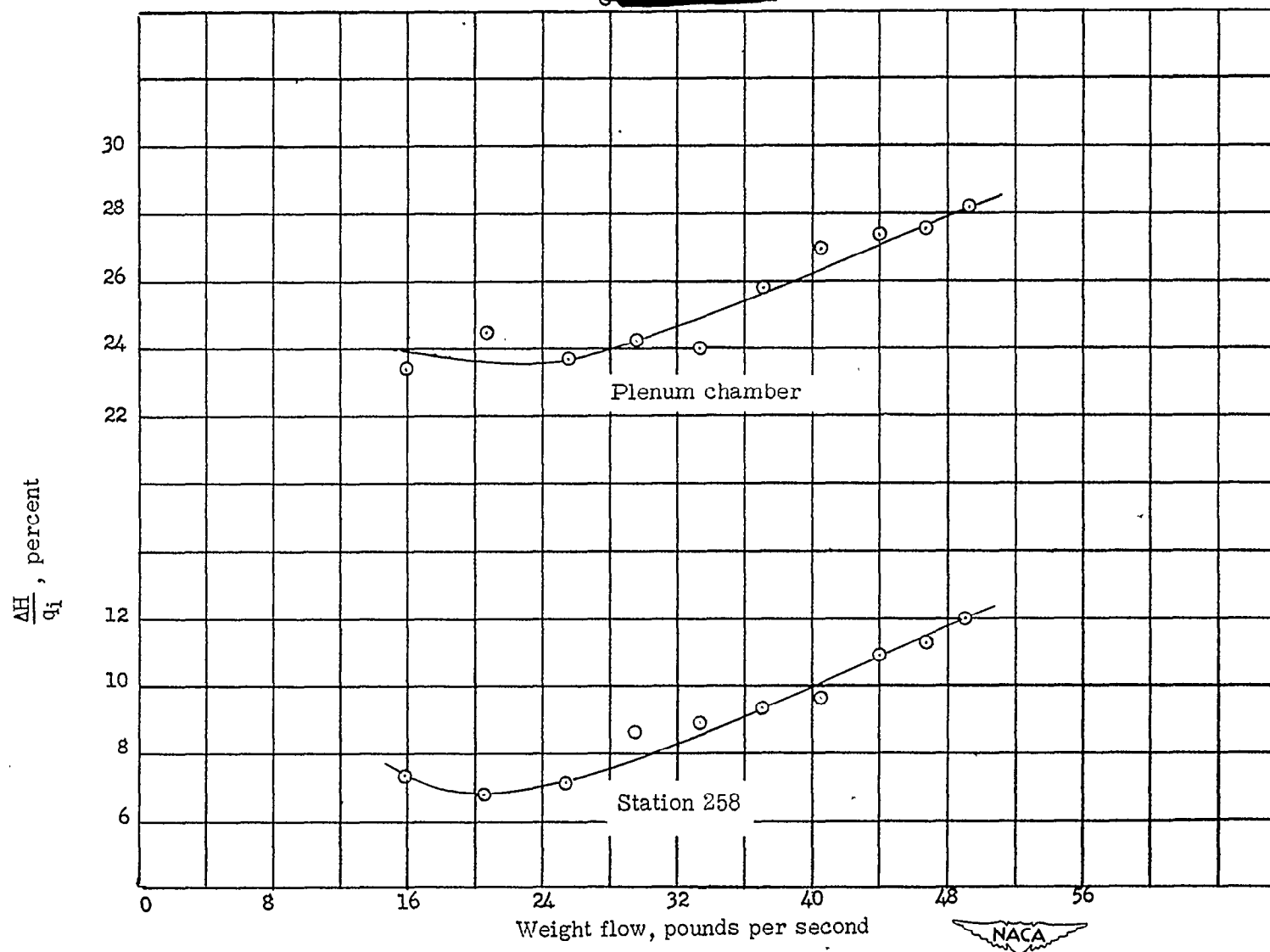
Figure 18.- Pressure-loss coefficient $\frac{\Delta H}{q_i}$ with duct in original condition. Half-duct.
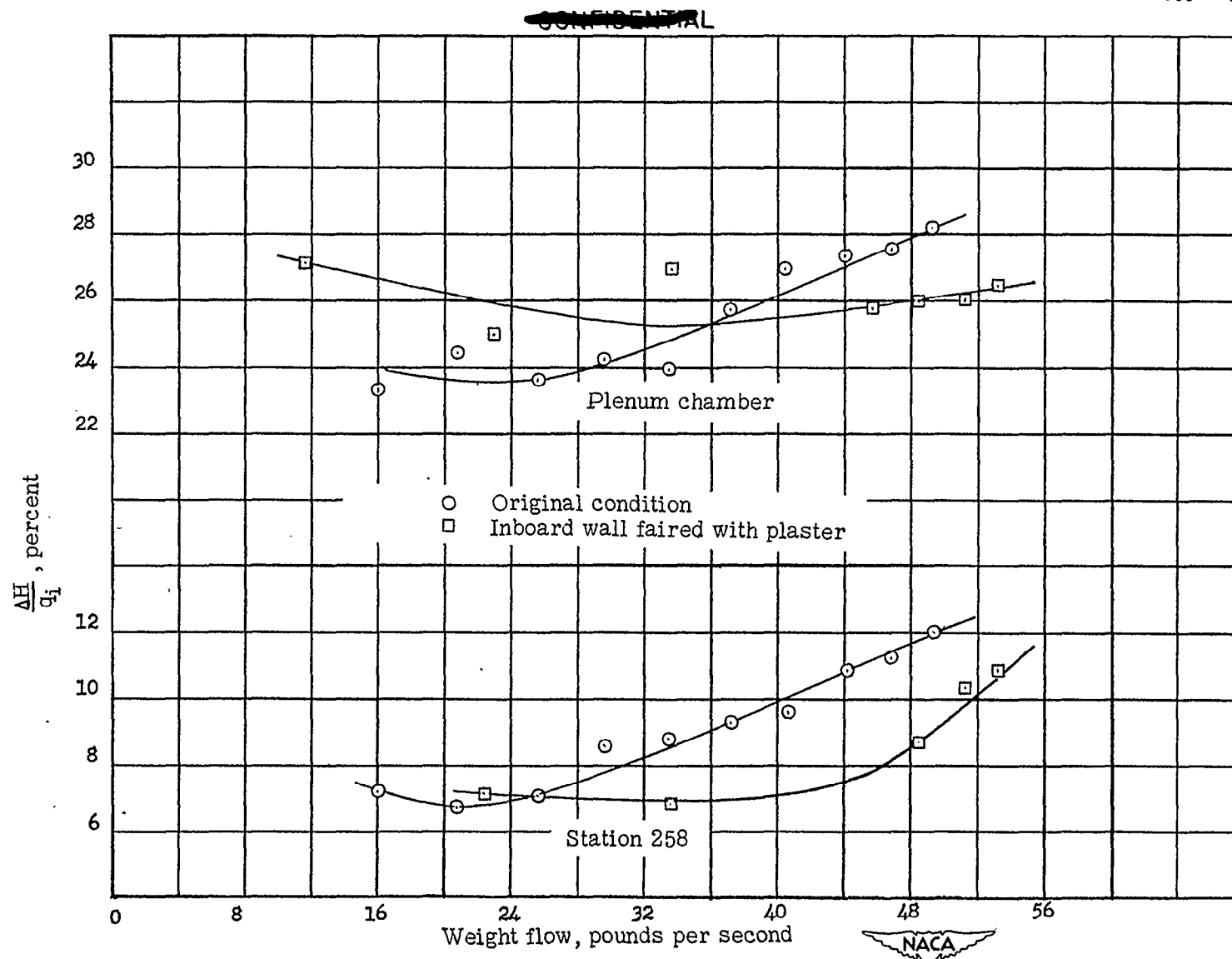
Figure 19.- Effect of refairing inboard wall on pressure-loss coefficient $\frac{\Delta H}{q_i}$. Half-duct.
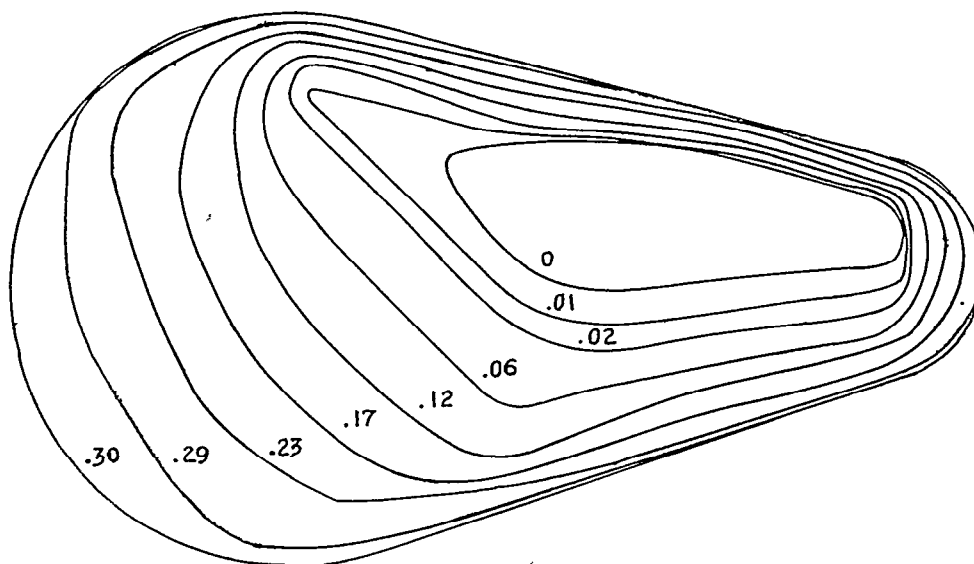
Original condition. $\frac{\Delta H}{q_i}$, 12 percent; air weight flow, 49 pounds per second.

Inboard

Outboard

NACA
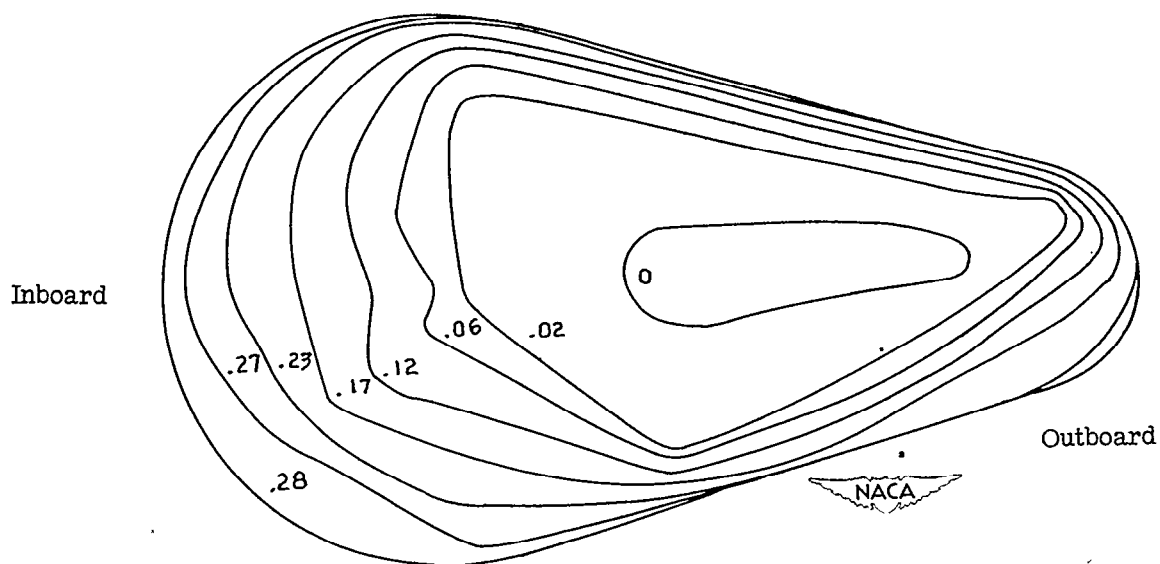
Refaired duct. $\frac{\Delta H}{q_i}$, 10 percent; air weight flow, 53 pounds per second.

Figure 20.- Contours of loss coefficient at station 258 for original and refaired conditions. Half-duct.
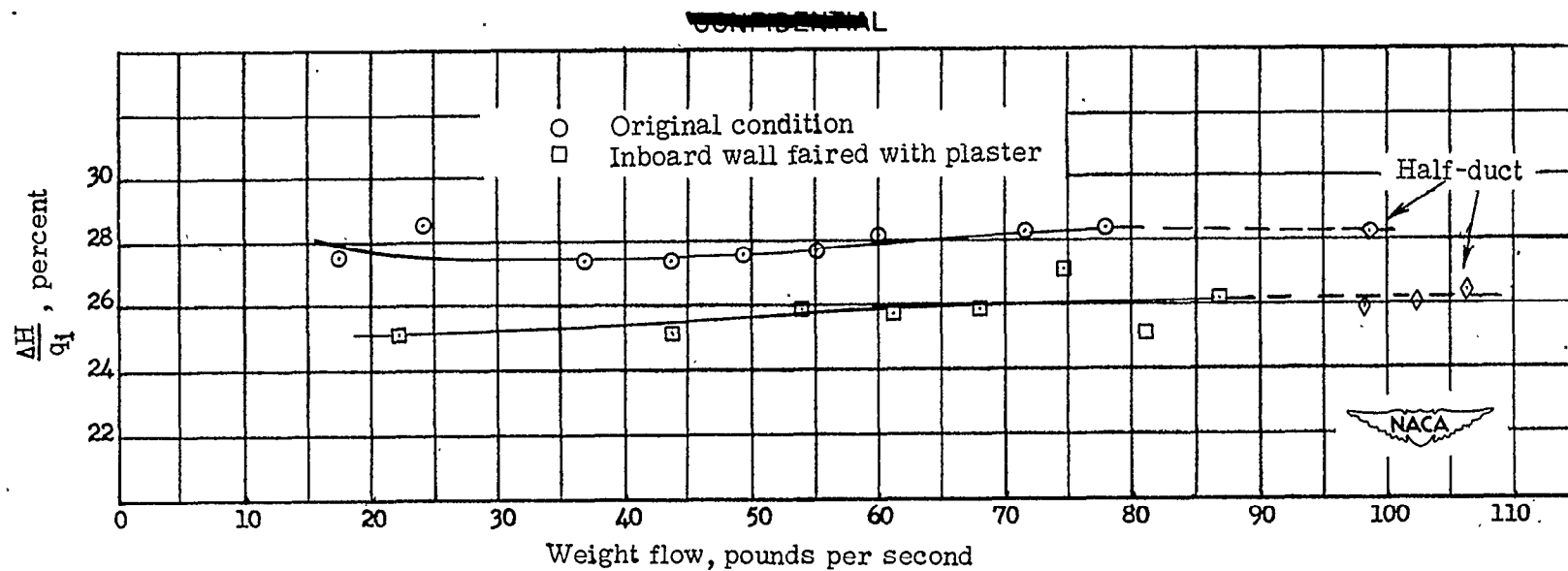
Figure 21.- Effect of fairing inboard wall on pressure-loss coefficient $\frac{\Delta H}{q_i}$ at plenum chamber. Complete duct.
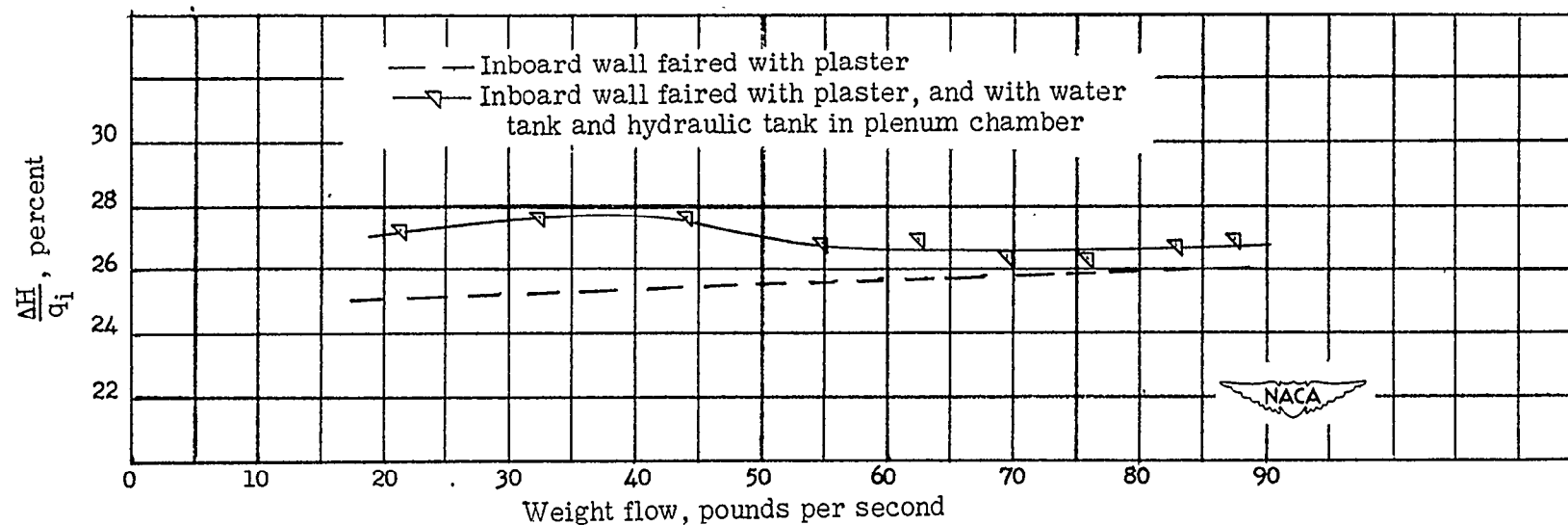
Figure 22.- Effect of installation of hydraulic tank and water tank on pressure-loss coefficient $\dfrac{\Delta H}{q_i}$ at plenum chamber. Complete duct.
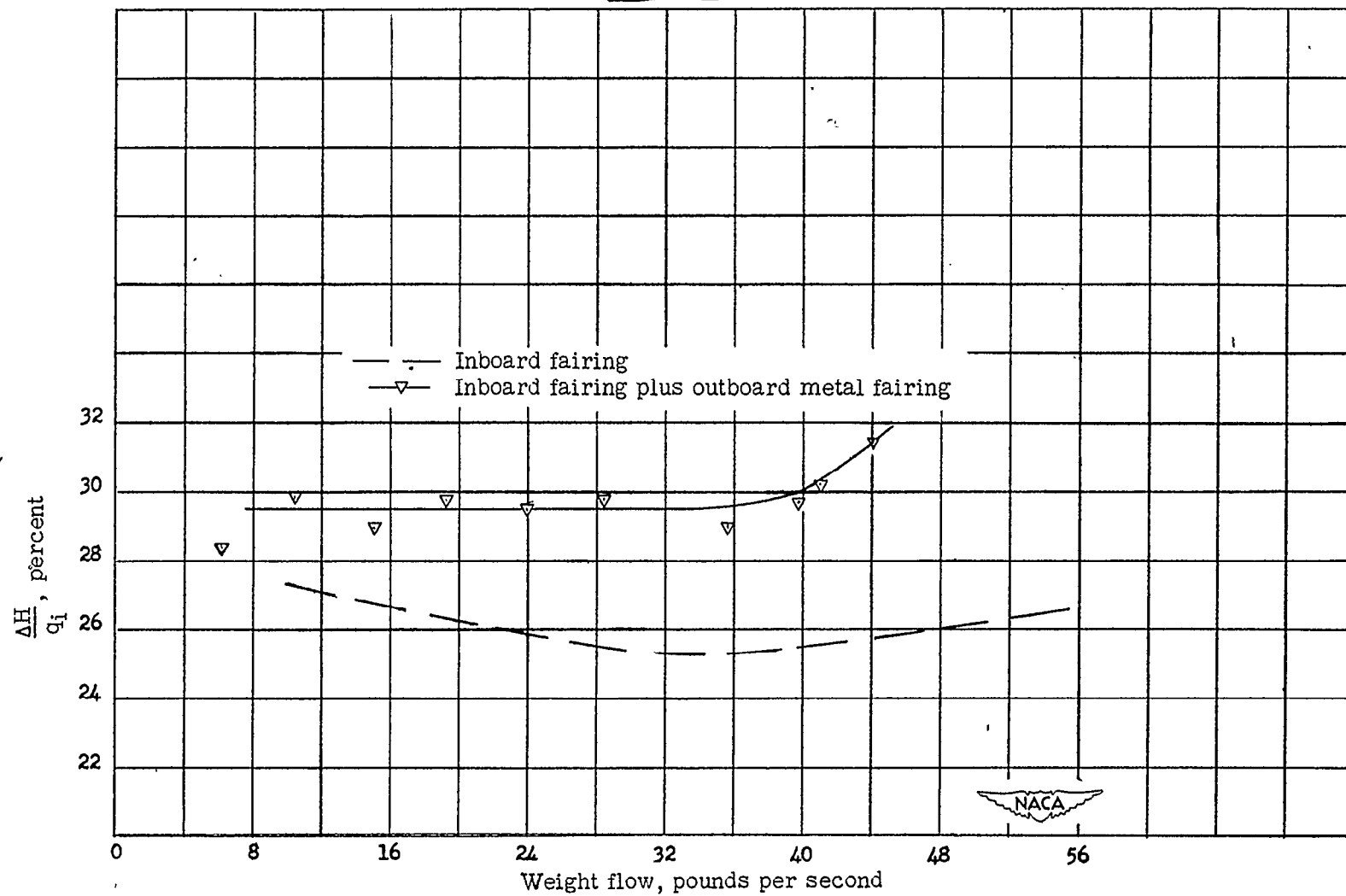
Figure 23.- Effect of outboard metal fairing on pressure-loss coefficient $\frac{\Delta H}{q_i}$ at plenum chamber. Half-duct.
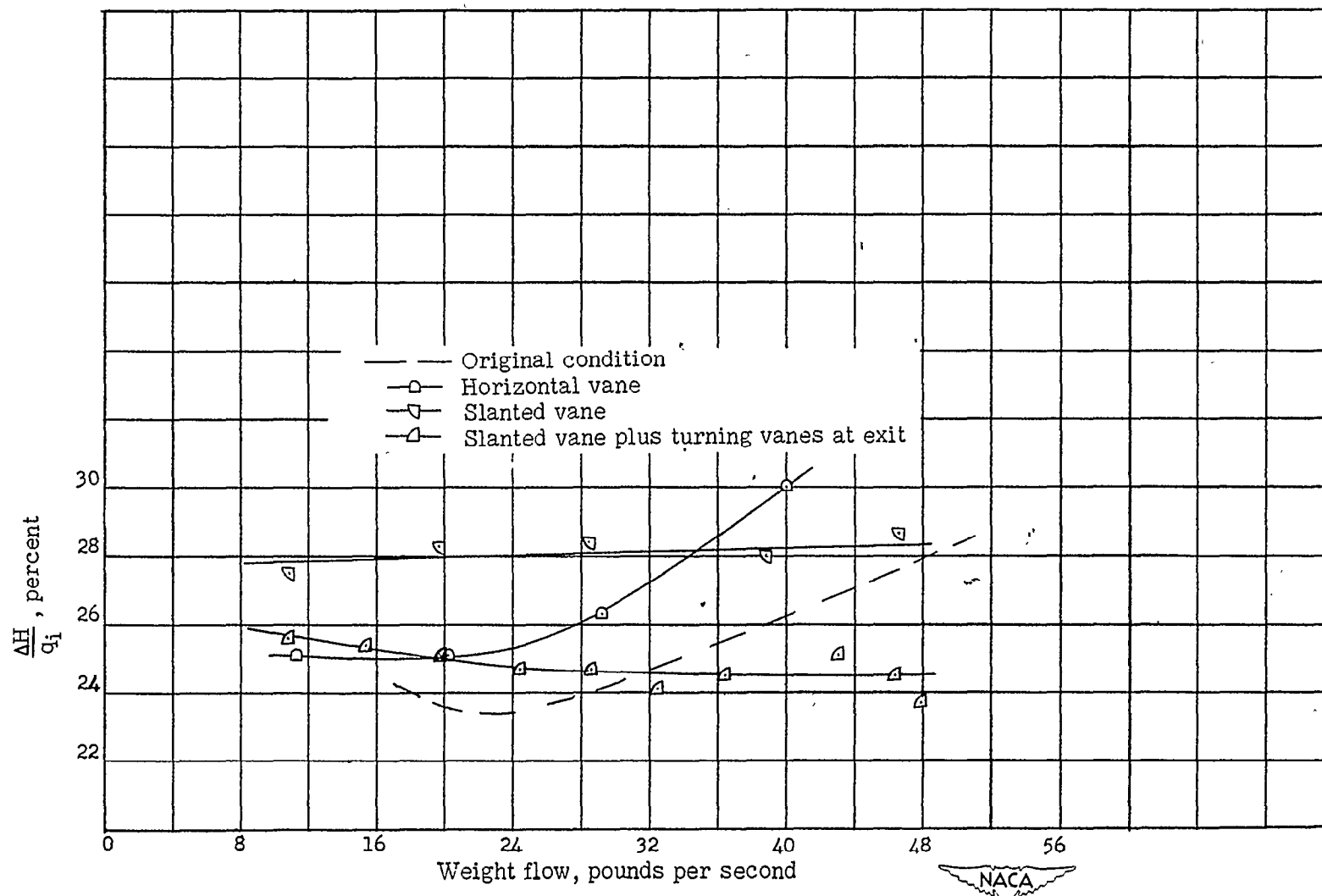
Figure 24.- Effect of different vane combinations on pressure-loss coefficient $\frac{\Delta H}{q_i}$ at plenum chamber. Half-duct.
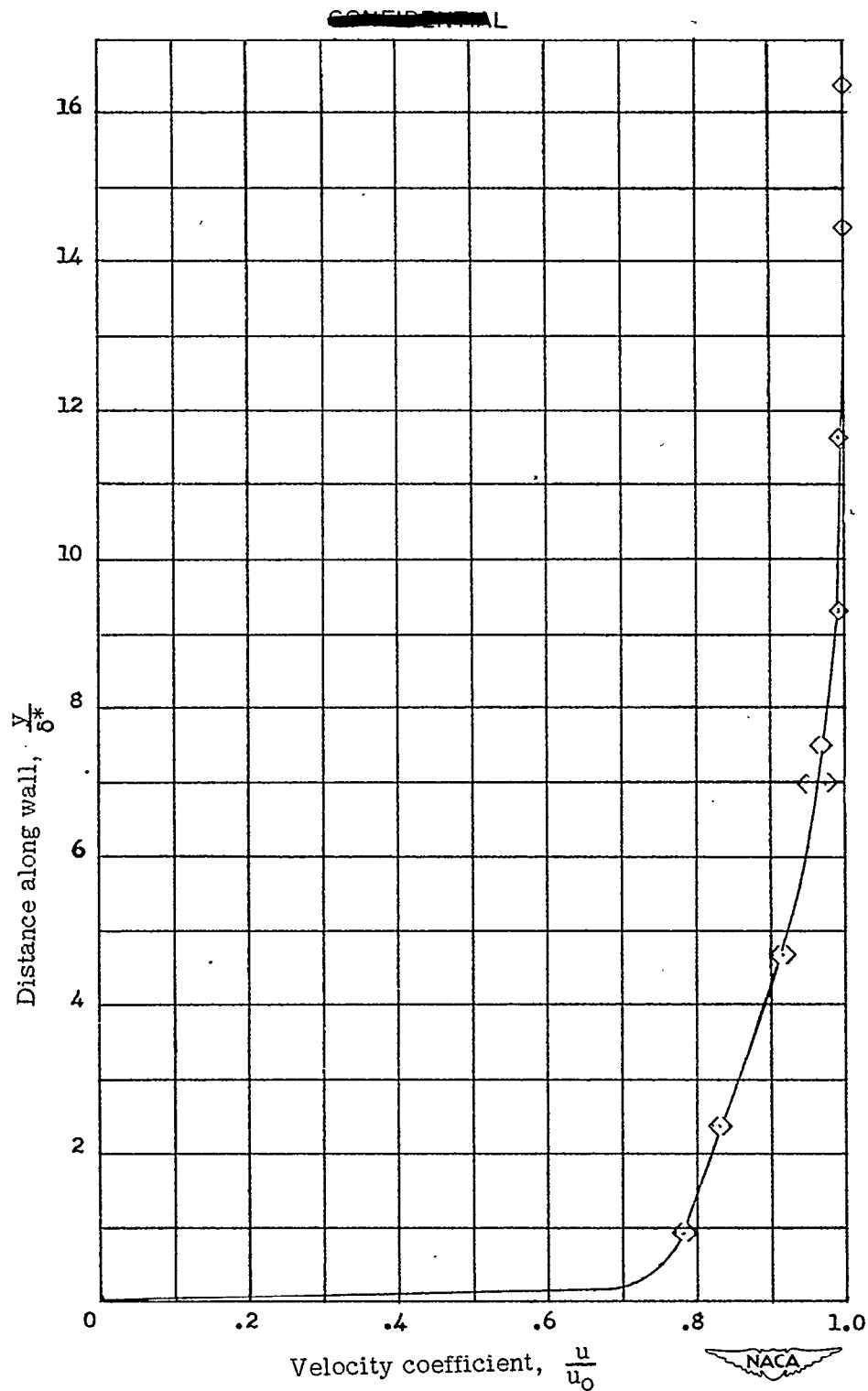
CONFIDENTIAL

Figure 25.- Boundary-layer velocity profile for $1\frac{1}{2}$-inch boundary layer. Extended symbols indicate spread of data at different velocities. Air-flow range, from 15 to 85 pounds per second.
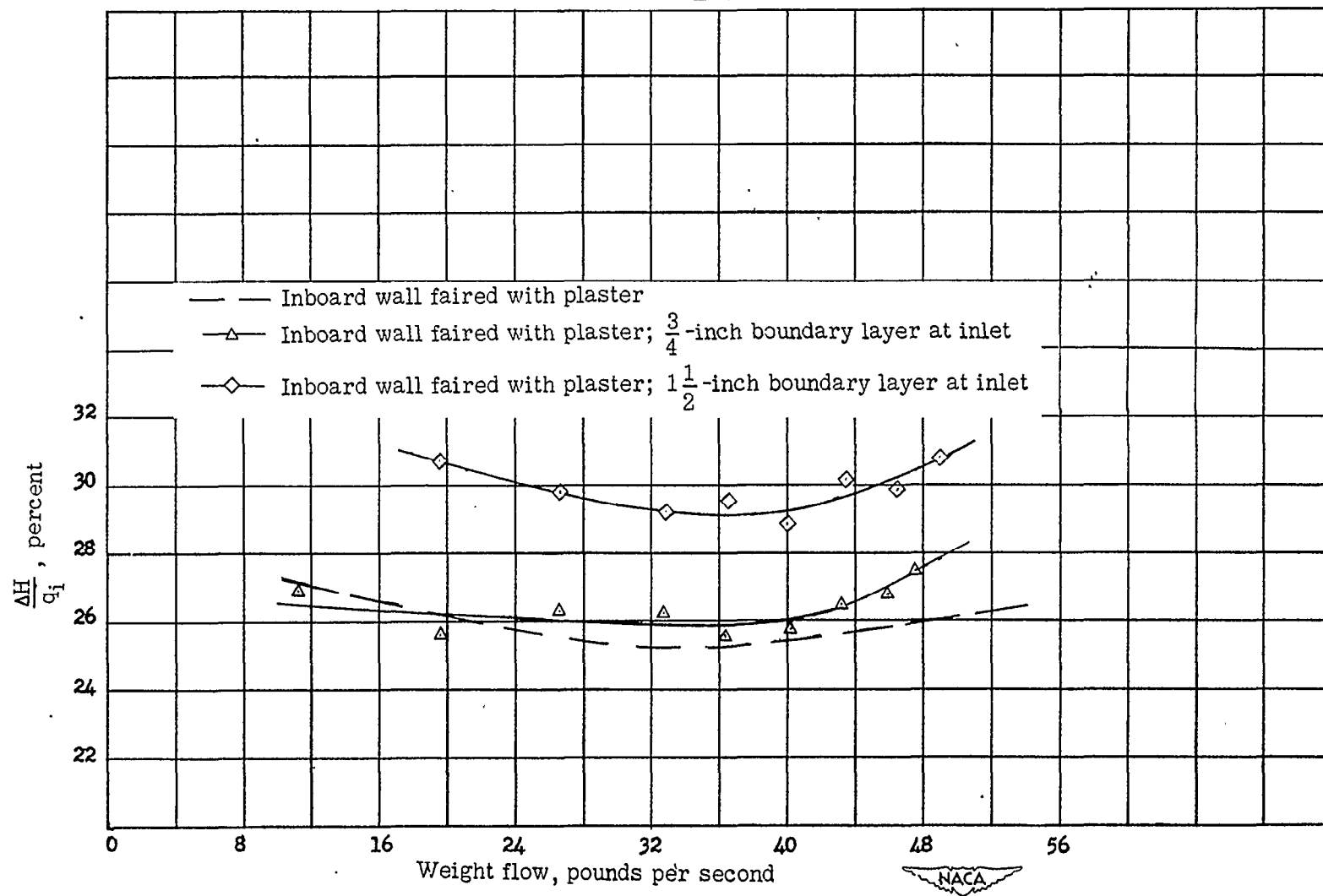
CONFIDENTIAL

Figure 26.- Effect of boundary layer on pressure-loss coefficient $\dfrac{\Delta H}{q_i}$ at plenum chamber. Half-duct.

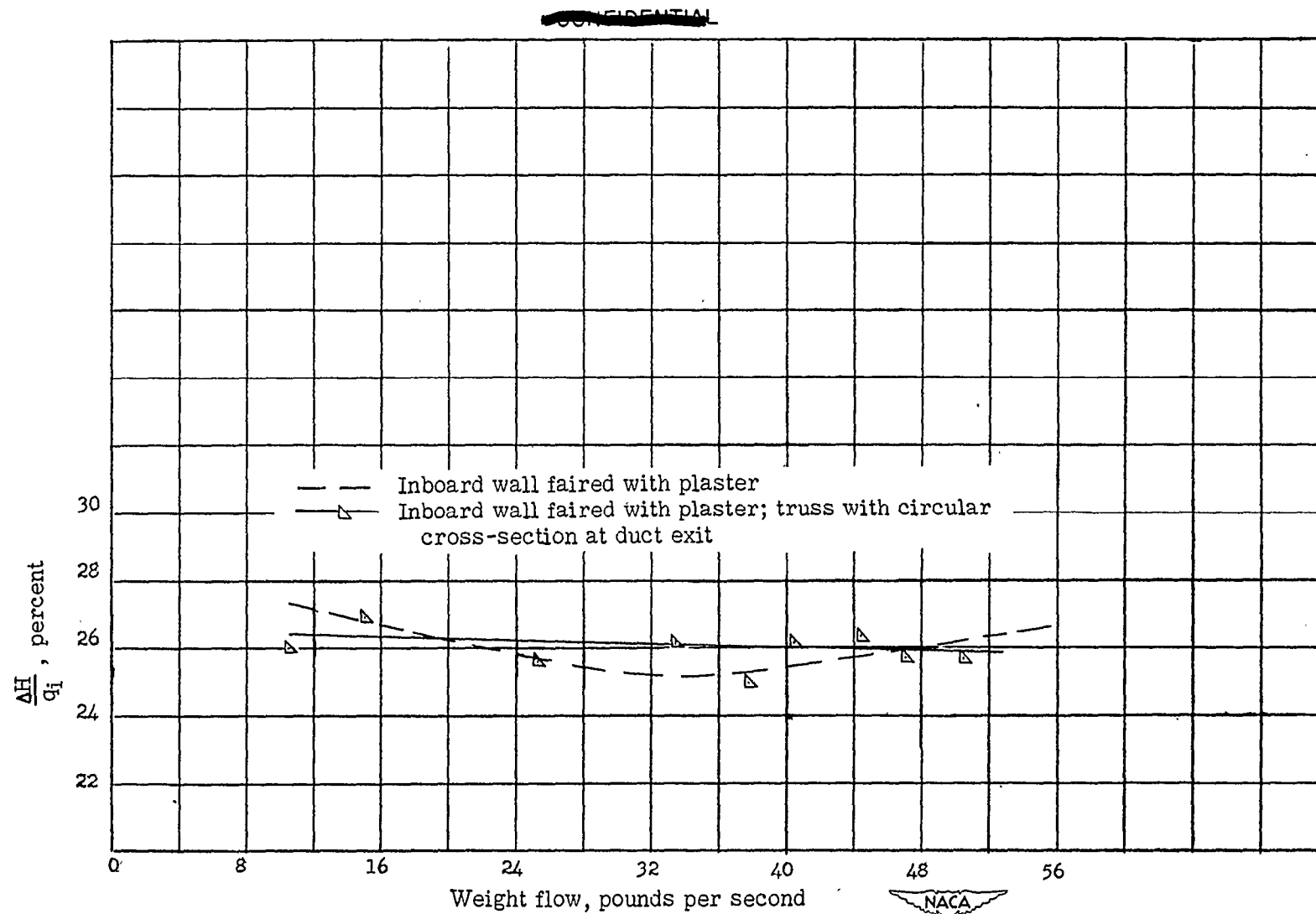Figure 27.- Effect of truss at duct exit on pressure-loss coefficient $\dfrac{\Delta H}{q_i}$ at plenum

chamber. Half-duct.

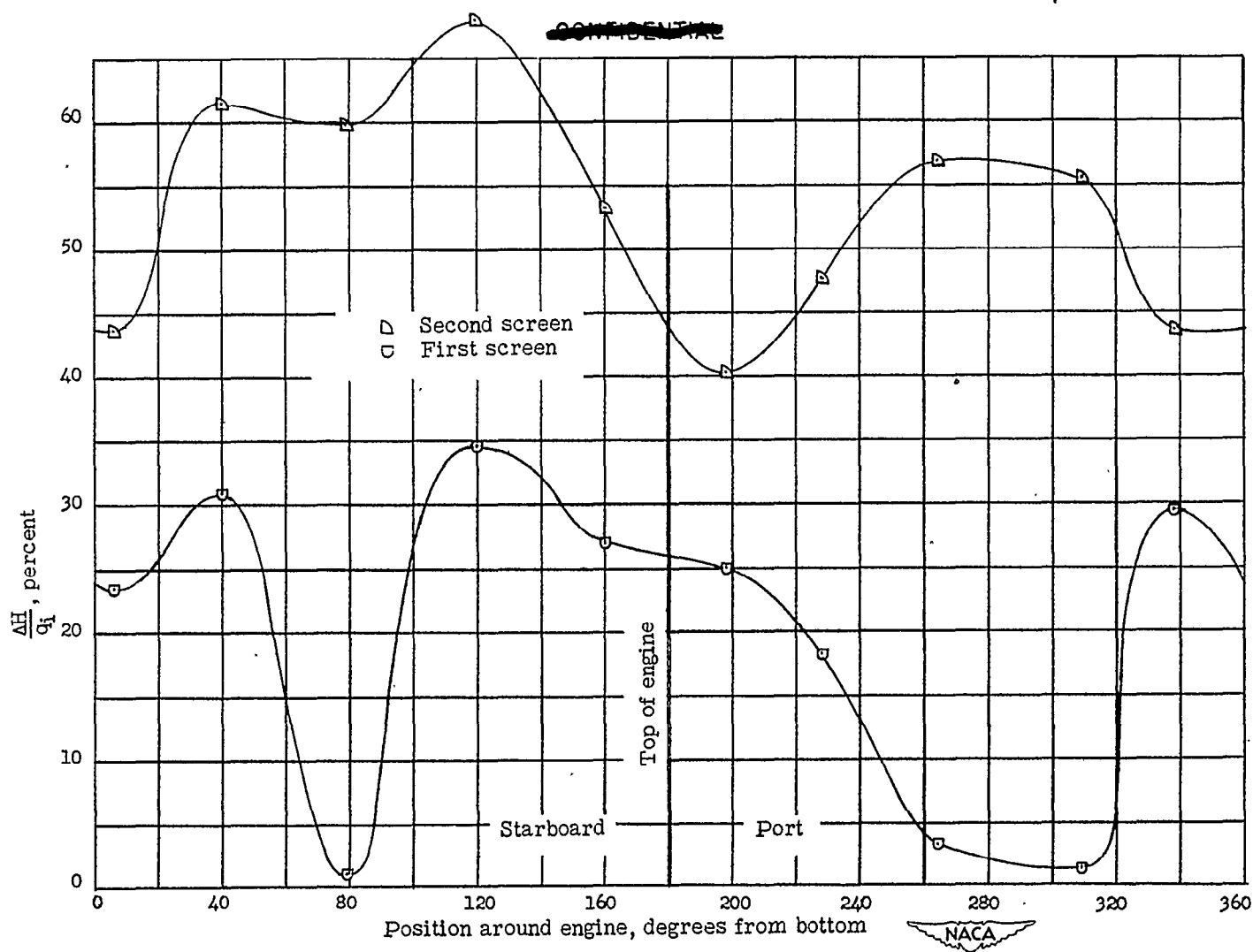Inboard wall faired with plaster
Inboard wall faired with plaster; truss with circular cross-section at duct exit

$\dfrac{\Delta H}{q_i}$, percent

Weight flow, pounds per second

Figure 28.- Typical pressure-loss distribution around engine. Air flow, 86.5 pounds per second.